

# INFLUENCE OF SHADING ON I-V CHARACTERISTICS OF THIN FILM PV MODULES

## VPLIV SENČENJA NA I-U KARAKTERISTIKO TANKOPLASTNIH FOTONAPETOSTNIH MODULOV

Matej Žnidarec<sup>✉</sup>, Danijel Topić<sup>1</sup>, Josip Bušić<sup>1</sup>

**Keywords:** Shading, thin-film PV module, amorphous silicon, copper-indium-selenide, I-V characteristic, P-V characteristic, power losses, efficiency

### **Abstract**

Photovoltaic (PV) systems are, numerically, the most widespread type of power plant that harvests renewable energy sources for electricity production. This paper investigates the influence of shading on the electrical characteristics of thin-film PV modules. Two types of thin-film PV modules are used: amorphous silicon and copper-indium-selenide. The electrical parameters of PV modules under various cases of shading are measured, analysed, and presented in tables and charts. A comparison between the electrical characteristics of crystalline silicon and thin-film PV modules under shading showed that thin-film PV modules have more consistent electrical parameters. I-V and P-V characteristics of shape of thin-film PV module are unaffected by shading. The power losses and efficiency of shaded modules are decreasing in linear relation to the increasing shaded area of a PV module.

✉ Corresponding author: Matej Žnidarec MEng, Faculty of Electrical Engineering, Computer Science and Information Technology Osijek, Department of Power Engineering, Kneza Trpimira 2B, 31000 Osijek, Tel.: +385 91 255 1520, E-mail address: [mznidarec@etfos.hr](mailto:mznidarec@etfos.hr)

<sup>1</sup> Faculty of Electrical Engineering, Computer Science and Information Technology Osijek, Department of Power Engineering, Kneza Trpimira 2B, 31000 Osijek

## **Povzetek**

Fotonapetostni sistemi so številčno najbolj razširjena vrsta elektrarn, ki izkorišča obnovljivi vir energije za proizvodnjo električne energije. Članek obravnava vpliv senčenja na električne lastnosti tankoplastnih fotonapetostnih modulov. Uporabljata se dve vrsti tankoplastnih fotonapetostnih modulov, in sicer iz amornega silicija in bakra-indija selenid. V članku se tako merijo in analizirajo električni parametri fotonapetostnih modulov v okviru različnih primerov senčenja. Rezultati so predstavljeni tabelarično in grafično. Primerjava med električnimi lastnostmi silicijevih in tankoplastnih fotonapetostnih modulov v skladu s senčenjem je pokazala, da imajo tankoplastni fotonapetostni moduli bolj dosledne električne parametre. Senčenje ne vpliva na I-U in P-U karakteristike tankoplastnih modulov. Izgube in izplen v primeru senčenja modula se zmanjšuje linearno glede na vse večjo senčenje območja modula.

## **1 INTRODUCTION**

In the 21<sup>st</sup> century, humankind has encountered the problem of global warming because the vast majority of electricity is produced from fossil fuels. According to World Energy Statistics 2016, published by the International Energy Agency, global energy needs can be satisfied by coal only until 2088. Oil reserves will be exhausted by 2060 but, even worse, natural gas reserves will be exhausted by 2053, [1]. Pollution and the climate changes that the usage of fossil fuels are bringing are even more noticeable. During the 1990s, scientists observed rapid changes of global temperature and climate changes, [2]. The response to that was the first attempt to tackle the problems with the Kyoto Protocol, in which world leaders committed their country to reduce gas emissions into the atmosphere, [3]. In 2007, the European Union responded with the 2020 Climate & energy package in which a set of binding legislation ensures that the EU meets its climate and energy targets for the year 2020. Three key targets are a 20% cut in greenhouse emissions from 1990 levels, a 20% improvement in energy efficiency and 20% of EU energy from renewable energy sources i.e. solar energy, wind power, hydropower, geothermal energy and bio-energy, [4]. The framework adopted by EU leaders in October 2014 that builds on the 2020 climate & energy package is the 2030 climate & energy framework with key targets of a 40% cut in greenhouse emission, a 27% improvement in energy efficiency, and 27% of EU energy from renewables, [5]. The ultimate goal for 2050 is a low-carbon economy in which the EU has cut greenhouse gas emissions to 80% below 1990 levels, [6]. Photovoltaic systems (PV) are the most widespread form of harvesting solar energy for electricity production. There are two main types of solar cell technologies used today: crystalline silicon and thin film photovoltaics. Electrical characteristics of solar cells are represented with *I-V* and *P-V* characteristics. The output of a PV module depends directly on input energy from the sun and the temperature of a PV module. If even a small part of irradiated energy is shaded by an object, the output energy of a PV module is significantly reduced, [7].

In [8], the shading influence on the *I-V* characteristic of a mono-crystalline PV module was studied. The results show that power loss depends on the location of the shade on the PV module. If a shade is placed across all six columns of PV cells, horizontally, power decreases by approximately 93%. If a shade is placed across 6 cells in one column, vertically, power decreases by approximately 30%; this does not depend on the number of shaded cells in the same column. Zulu and Kashweka, [9], conducted an experiment of shading of a monocrystalline PV module in three steps, 25%, 50% and 75% of the area. Results showed that in the case of 25% of area shaded, power output was reduced by 75% and efficiency dropped to approximately  $(2.9\% \pm 0.2\%)$ . In the

case of 50% and 75% of the area of module shaded, power output dropped by 90 % and efficiency dropped to approximately  $0.8\% \pm 0.1\%$ . Sun et al., [10], were studying the influence of wire pole shading on electrical properties of six polycrystalline PV modules. The results showed that the power output of modules depends on the number of bypass diodes integrated into the PV module, the size of the shaded area, and the position of the shadow on the PV module surface. Dolara et al., [11], studied the influence of different shading scenarios on monocrystalline and polycrystalline silicon single-cell and whole PV modules. They conducted two shading scenarios for single-cell, right-to-left and bottom-to-top. For a PV module, three shading scenarios were examined: horizontal, vertical and diagonal. A decrease of the power output for every case conducted in this paper does not depend on crystalline technology of which PV modules are made. In [12], [13], [14], [15] and [16], the effects of partial shading on PV arrays characteristics and efficiency are investigated. The main goal of the papers was to propose Maximum Power Point Tracker algorithms, which would extract maximum power from partially shaded PV modules with deformed  $P$ - $V$  characteristics. Bai et al., [17], proposed new physical PV array arrangements to mitigate partial shading effects. Three new physical arrangements are proposed and compared with the performance of existing configurations. While, according to [18], the efficiency and production of thin-film modules is increasing, researchers are neglecting the investigation of this kind of photovoltaics.

This paper investigates influence of shading on electrical characteristics of thin-film PV modules unlike other research studies so far, which only examined crystalline silicon technologies of PV modules.

## 2 METHODOLOGY

### 2.1 Measuring method and instruments

Experiments were conducted on two different technologies of thin film PV modules. The first PV module, named Masdar MPV100-S, uses amorphous silicon technology for electricity production. The second PV module, named Solar Frontier SF150-S, uses copper-indium-selenide (CIS) alloy for electricity production. The technical specifications of Masdar MPV100-S are shown in Table 1, [19, 20].

**Table 1:** Masdar MPV100-S and Solar Frontier SF150-S technical specifications

Parameter	Unit	Masdar MPV100-S	Solar Frontier SF150-S
Nominal peak power ( $P_{MPP}$ )	W	100	150
Nominal voltage ( $V_{MPP}$ )	V	75	81.5
Nominal current ( $I_{MPP}$ )	A	1.34	1.85
Open circuit voltage ( $V_{OC}$ )	V	96	108
Short-circuit current ( $I_{SC}$ )	A	1.56	2.2

Efficiency ( $\eta$ )	%	7	12.2
Temperature coefficient of $P_{MP}$	%/°C	- 0.2	- 0.31
Temperature coefficient of $V_{OC}$	%/°C	- 0.3	- 0.3
Temperature coefficient of $I_{SC}$	%/°C	0.1	0.01
Dimensions (length x width x thickness)	mm	1300×1100×7	1257×977×35
Weight	kg	29.5	20

The measuring instruments used for the experiments were a Metrix PX110 Powermeter, a Peaktech 3320 DMM, and a Seaward SOLAR Survey 200. The Metrix PX 110 Powermeter is a digital power meter and it is used for measuring the voltage, current and output power of a PV module. The electrical circuit used for measuring the  $I$ - $V$  characteristics of the PV modules is shown in Figure 1.

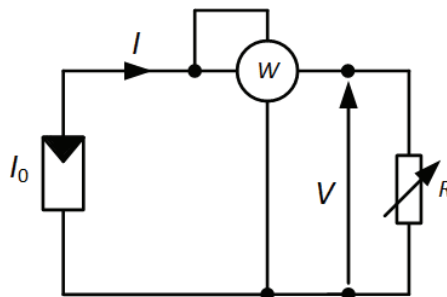


**Figure 1:**  $I$ - $V$  characteristic measuring electrical circuit

A Peaktech 3320 DMM Digital multimeter is used for measuring short-circuit current and open-circuit voltage of the PV modules while a Seaward SOLAR Survey 200 instrument is used for measuring the solar irradiance in  $W/m^2$ .

## 2.2 Shading simulation

The simulated shading profile is divided into 11 steps from the bottom of the module to the top. The first step of the shading profile spreads from the first 10 cm from the bottom edge of the PV module across its whole width. Each next step adds another 10 cm in the height of the module. The final and 11<sup>th</sup> step shades 110 cm of the module from the bottom edge to the top, leaving only small part of unshaded area, which depends on the height of the PV module. Measurement of the  $I$ - $V$  characteristic for each PV module and for every shading case was done according to the electrical schematic shown in Figure 1. The first  $I$ - $V$  characteristic measuring was done for an unshaded area of a PV module. After that, eleven  $I$ - $V$  characteristics for each PV module are measured for each shading case. At the same time as the  $I$ - $V$  characteristic is measured, the

irradiance level was measured. An example of the 1<sup>st</sup>, 2<sup>nd</sup> and 11<sup>th</sup> steps of the shading profile is presented in Figure 2.

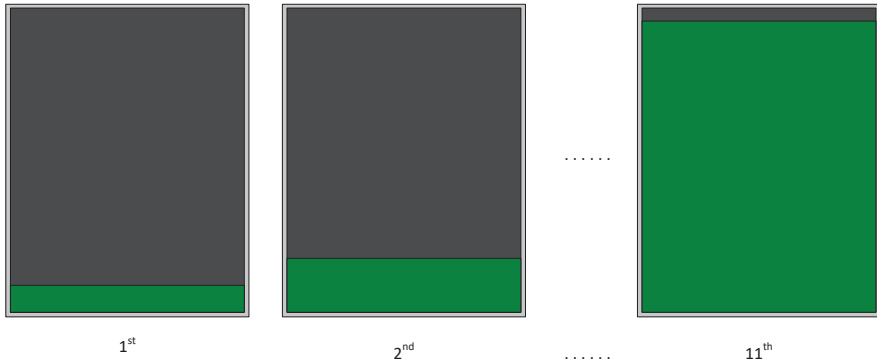


**Figure 2:** First, second and 11<sup>th</sup> steps of the shading profile

### 3 RESULTS

#### 3.1 Masdar MPV100-S

*I-V* and *P-V* characteristics for unshaded and 11 steps of shading profile for a Masdar MPV100-S amorphous silicon PV module are given in Figure 3 and Figure 4. The results reveal that *I-V* and *P-V* characteristic's shape does not depend on shading of PV module surface unlike mono- and polycrystalline silicon PV modules. The *P-V* characteristics given in Figure 4 have only one maximum, regardless of shading case.

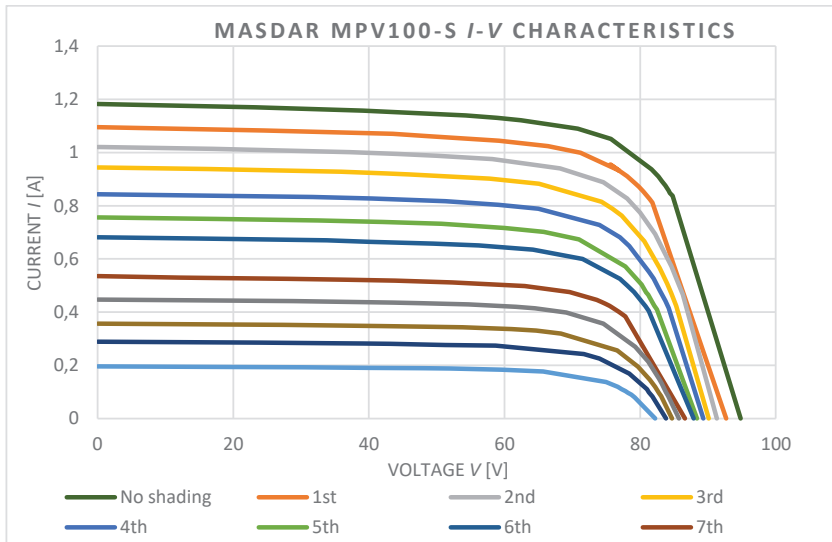


**Figure 3:** *I-V* characteristics for unshaded and 11 shading cases of Masdar MPV100-S PV module

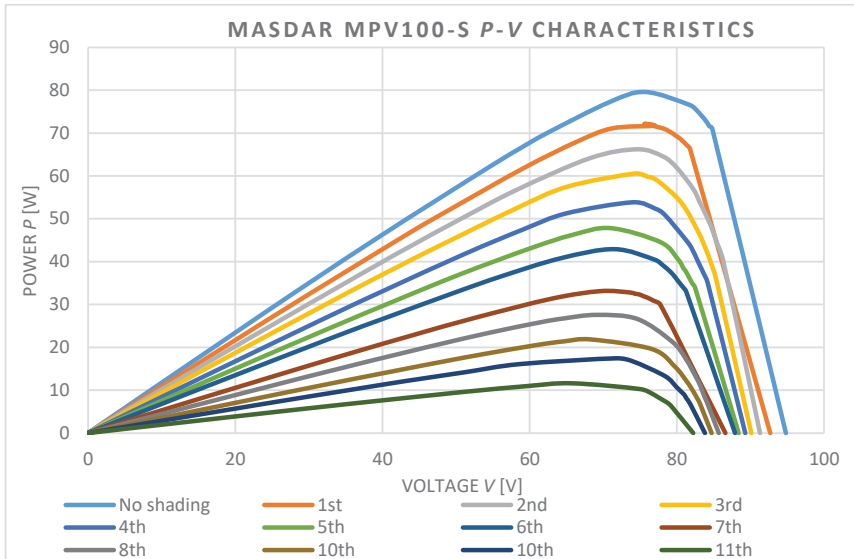


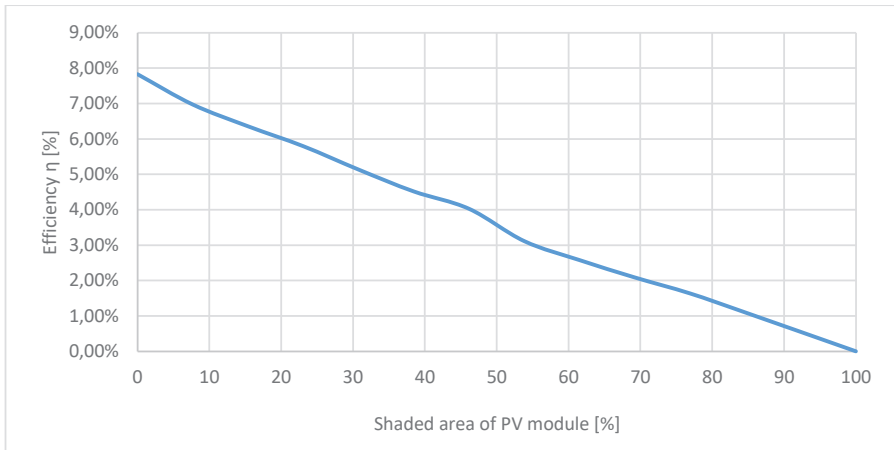
**Figure 4:** P-V characteristics for unshaded and 11 shading cases of Masdar MPV100-S PV module

The processed results for the Masdar MPV100-S PV module for unshaded and 11 cases of shading profile are given in Table 2. The results displayed in Table 2 show that the fill factor  $F$  of the  $I$ - $V$  characteristic does not change in a significant way, regardless of the shading case, which confirms that its shape is not significantly affected.

**Table 2:** Results for Masdar MPV100-S PV module

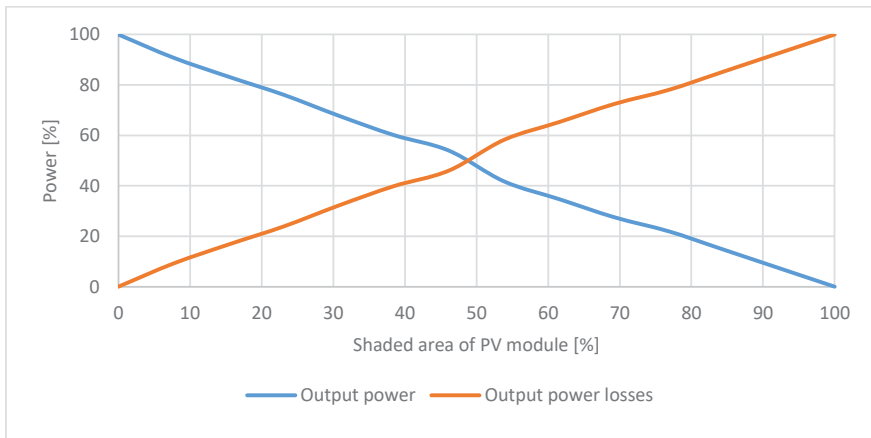
Shading case	Shadow height [cm]	Shaded area of PV module [%]	Output power of shaded PV module $P_n$ [W]	Output power loss $P_L$ [W]	Fill factor $F$ [%]
No shade	0	0	79.5	0	70.95
1 <sup>st</sup>	10	7.69	72.2	7.3	71.06
2 <sup>nd</sup>	20	15.38	66.2	13.3	71.02
3 <sup>rd</sup>	30	23.08	60.5	19.0	71.13
4 <sup>th</sup>	40	30.77	53.9	25.6	71.6
5 <sup>th</sup>	50	38.46	47.8	31.7	71.52
6 <sup>th</sup>	60	46.15	42.9	36.6	71.67
7 <sup>th</sup>	70	53.85	33.2	46.3	71.66
8 <sup>th</sup>	80	61.54	27.6	51.9	72.05
9 <sup>th</sup>	90	69.23	21.9	57.6	72.43
10 <sup>th</sup>	100	76.92	17.4	62.1	71.85
11 <sup>th</sup>	110	84.61	11.6	67.9	72

Figure 5 shows the relation of the Masdar MPV100-S PV module efficiency and shaded area of PV module surface. The curve shows that the efficiency of the PV module is linearly declining with the increase of the shaded area. Small deviations from the linear relation of the sizes are caused by measuring instrument error.



**Figure 5:** Efficiency of Masdar MPV100-S PV module in relation with shaded area

Output power and output power losses of the Masdar MPV100-S PV module in relation with the shaded area is given in Figure 6. Curves presented in the chart are showing that output power and output power losses of the PV module are inversely proportional and in linear relation to the increasing shaded area of a PV module. Small deviations from the linear relation are caused by measuring instrument error.



**Figure 6:** Output power and output power losses of Masdar MPV100-S in relation with shaded area

### 3.2 Solar Frontier SF150-S

Figure 7 and Figure 8 show  $I$ - $V$  and  $P$ - $V$  characteristics for unshaded and 11 steps of the shading profile for the CIS PV module Solar Frontier SF150-S. The results in Figure 7 and Figure 8 show that the shape of  $I$ - $V$  and  $P$ - $V$  characteristics are not influenced by the shading case of the PV module. The  $P$ - $V$  characteristics given in Figure 8 have only one maximum regardless of the shading case

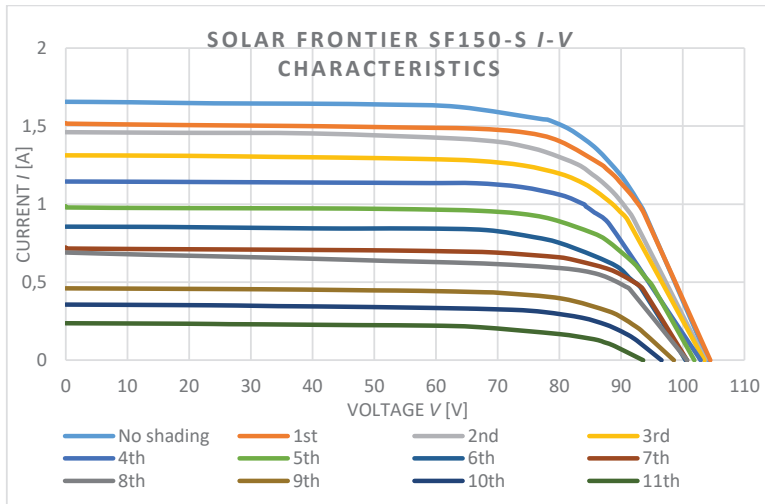


**Figure 7:**  $I$ - $V$  characteristics for unshaded and 11 shading cases of Masdar Solar Frontier SF150-S module

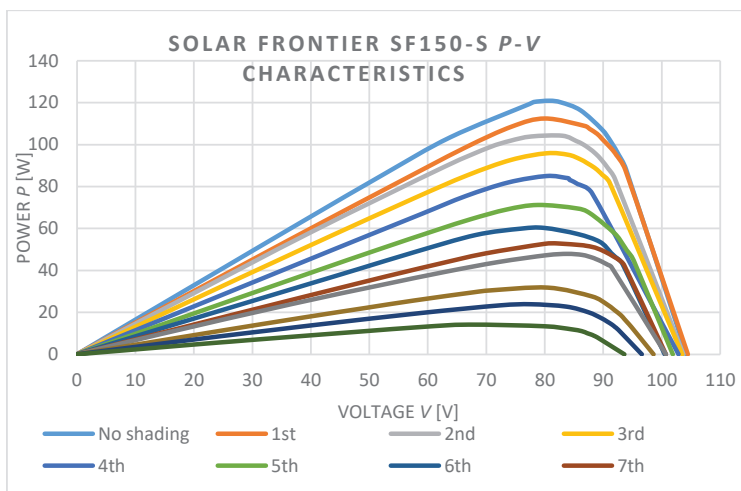


**Figure 8:**  $P$ - $V$  characteristics for unshaded and 11 shading cases of Masdar Solar Frontier SF150-S module



The processed results for Solar Frontier SF150-S PV module for unshaded and 11 cases of shading profile are given in Table 3. As in the former case, fill factor  $F$  is showing that shape of the  $I$ - $V$  characteristic is not significantly affected by the shading.

**Table 3: Results for Solar Frontier SF150-S PV module**

Shading case	Shadow height [cm]	Shaded area of PV module [%]	Output power of shaded PV module $P_n$ [W]	Output power loss $P_L$ [W]	Fill factor $F$ [%]
No shade	0	0	120.9	0	70.11
1 <sup>st</sup>	10	7.96	112.4	8.5	70.76
2 <sup>nd</sup>	20	15.91	104.2	16.7	68.73
3 <sup>rd</sup>	30	23.87	95.9	25.0	70.57
4 <sup>th</sup>	40	31.82	84.9	36.0	72.06
5 <sup>th</sup>	50	39.78	71.2	49.7	70.79
6 <sup>th</sup>	60	47.73	63.0	57.9	73.23
7 <sup>th</sup>	70	55.69	53.0	67.9	72.8
8 <sup>th</sup>	80	63.64	47.9	73.0	69.04
9 <sup>th</sup>	90	71.56	31.9	89.0	70.18
10 <sup>th</sup>	100	79.55	23.9	97.0	69.5
11 <sup>th</sup>	110	87.51	16.0	104.9	72.43

The relation of Solar Frontier SF150-S PV module efficiency and the shaded area of the PV module surface is shown in Figure 9. The curve shows that efficiency of the PV module is declining linearly with the increase of the shaded area. Small deviations from the linear relation of the sizes are caused by measuring instrument error.

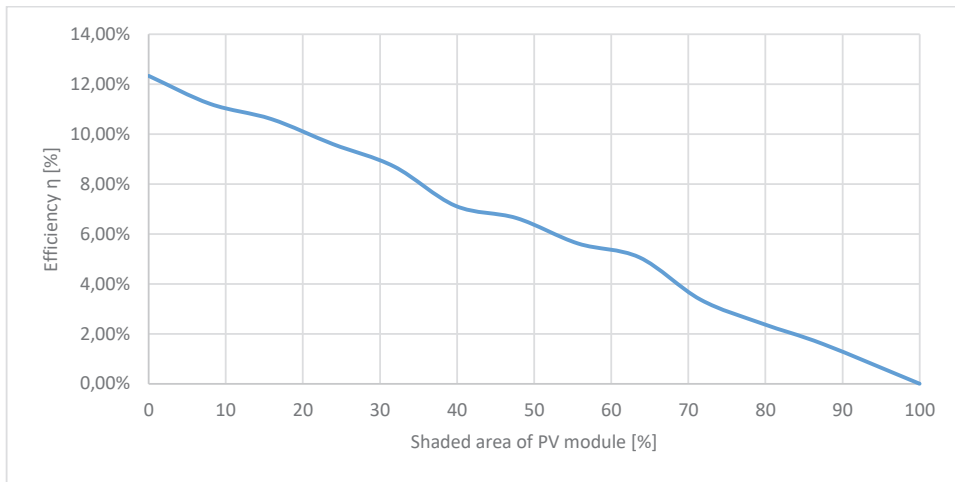


**Figure 9:** Efficiency of Solar Frontier SF150-S module in relation with shaded area

Figure 10 shows output power and output power losses of Solar Frontier SF150-S module in relation with the shaded area. Curves plotted in the chart are showing that output power and output power losses of the PV module are inversely proportional and in linear relation to the increasing shaded area of a PV module. Small deviations from the linear relation are caused by measuring instrument error.

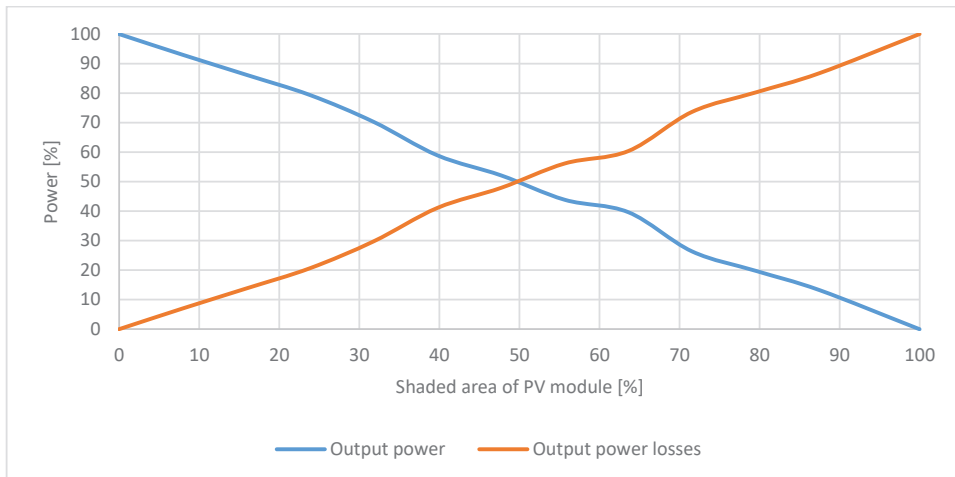


**Figure 10:** Output power and output power losses of Solar Frontier SF150-S in relation with shaded area

## 4 CONCLUSION

This paper studied the influence of shading on electrical characteristics of thin-film PV modules (amorphous silicon and copper-indium-selenide). The influence on the electrical characteristics of the PV modules is measured, analysed and shown in charts and tables. The first difference in the electrical characteristics of crystalline silicon is visible from the shape of the  $I$ - $V$  and  $P$ - $V$  curves in a case of shading. The shape of the  $I$ - $V$  characteristic of thin-film PV modules is unaffected unlike crystalline silicon PV modules, which are drastically deformed. The  $P$ - $V$  curves of thin-film PV modules have only one maximum, regardless of shading case, unlike crystalline silicon PV modules, which could have a greater number of maximums depending on the number of bypass diodes and position and configuration of solar-cells. Thin-film PV modules can be observed as a single-cell electric generator but crystalline silicon PV modules cannot. They are a set of PV cells connected in series-parallel formation, with a certain number of bypass diodes integrated between them to reduce power losses, depending on the manufacturer. Therefore, if only a single-cell is shaded, its change of electrical characteristics affects the entire PV module. Power losses and efficiency of the thin-film modules are in a linear relation to the shaded area of the PV modules. Since the production price of thin-film photovoltaics is lower than crystalline silicon and the efficiency and production of PV modules is constantly increasing, PV systems based on thin-film photovoltaics are more likely to experience growth in newly installed PV systems. Furthermore, PV systems based on thin-film photovoltaics are more suitable for urban areas in which shading by buildings, utility poles, tree branches, and leaves is a much more common phenomenon than it is in rural areas.

## References

- [1] **International Energy Agency:** *Key World Energy Statistics* [online], 2016. Available: <https://www.iea.org/publications/freepublications/publication/KeyWorld2016.pdf> (12.12.2016)
- [2] **B. C. Black, G. J. Weisel:** *Global Warming*, Greenwood, 2010
- [3] **United Nations:** *Kyoto Protocol to the United Nations Framework Convention on Climate Change* [online], 1998. Available: <https://unfccc.int/resource/docs/convkp/kpeng.pdf> (12.12.2016)
- [4] **European Union:** 2020 climate & energy package [online]. Available: [http://ec.europa.eu/clima/policies/strategies/2020\\_en](http://ec.europa.eu/clima/policies/strategies/2020_en) (12.12.2016)
- [5] **European Union:** 2030 climate & energy framework [online]. Available: [http://ec.europa.eu/clima/policies/strategies/2030\\_en](http://ec.europa.eu/clima/policies/strategies/2030_en) (20.12.2016)
- [6] **European Union:** 2050 low-carbon economy [online]. Available: [http://ec.europa.eu/clima/policies/strategies/2050\\_en](http://ec.europa.eu/clima/policies/strategies/2050_en) (20.12.2016)
- [7] **G. M. Masters:** *Renewable and Efficient Electric Power Systems*, John Wiley & Sons, 2004
- [8] **S. Seme, G. Štumberger:** *Shading effects in the IU characteristic of a mono-crystalline PV module*, XII International PhD Workshop OWD 2010, Wisla, 2010

- 
- [9] **A. Zulu, G. Kashweka:** *The Influence of Artificial Light and Shading on Photovoltaic Solar Panels*, International Journal of Energy Engineering, Vol. 3, Iss. 1, p.p. 15-20, 2013
  - [10] **Y. Sun, X. Li, R. Hong, H. Shen:** *Analysis on the Effect of Shading on the Characteristics of Large-scale on-grid PV System in China* [online], Energy and Power Engineering, Vol. 5, p.p. 215-218, 2013. Available: [http://file.scirp.org/pdf/EPE\\_2013101513553018.pdf](http://file.scirp.org/pdf/EPE_2013101513553018.pdf) (13.12.2016)
  - [11] **A. Dolara, G. C. Lazaroiu, S. Leva, G. Manzolini:** *Experimental investigation of partial shading scenarios on PV (photovoltaic) modules*, Energy, Vol. 55, p.p. 466-475, 2013
  - [12] **A. I. Aldaoudeyeh:** *Photovoltaic-battery scheme to enhance PV array characteristics in partial shading conditions*, IET Renewable Power Generation, Vol. 10, Iss. 1, p.p. 108-115, 2016
  - [13] **B. Raja, M. R. Satheesh Kumar, S. Vikash, K. Hariharan:** *Maximum power point tracking in solar panels under partial shading condition using equilibration algorithm*, 2016 International Conference on Communication and Signal Processing (ICCSP), 2016
  - [14] **R. Dash, S. C. Swain, P. C. Panda:** *A study on the increasing in the performance of a solar photovoltaic cell during shading condition*, 2016 International Conference on Circuit, Power and Computing Technologies (ICCPCT), 2016
  - [15] **M. A. Ghasemi, H. M. Forushani, M. Parniani:** *Partial Shading Detection and Smooth Maximum Power Point Tracking of PV Arrays Under PSC*, IEEE Transactions on Power Electronics, Vol. 31, Iss. 9, p.p. 6281-6292, 2015
  - [16] **K. M. Tsang, W. L. Chan:** *Maximum power point tracking for PV systems under partial shading conditions using current sweeping*, Energy Conversion and Management, Vol. 93, p.p. 249-258, 2015
  - [17] **N. Belhaouasa, M. S. Ait Cheikhb, P. Agathoklisc, M. R. Oularbid, B. Amrouchea, K. Sedraouie, N. Djilali:** *PV array power output maximization under partial shading using new shifted PV array arrangements*, Solar Energy, Vol. 112, p.p. 41-54, 2015
  - [18] **Fraunhofer Institute for Solar Energy Systems:** *Photovoltaics report* [online], 2016. Available: <https://www.ise.fraunhofer.de/de/downloads/pdf-files/aktuelles/photovoltaics-report-in-englischer-sprache.pdf> (20.12.2016)
  - [19] **Masdar PV:** *MPV-S - Our a-Si Thin-Film PV Module* [online]. Available: [http://www.secondsol.de/index.php?page=ad\\_showup&ID\\_AD\\_UPLOAD=6630](http://www.secondsol.de/index.php?page=ad_showup&ID_AD_UPLOAD=6630) (15.12.2016)
  - [20] **Solar Frontier:** *Product overview SF145-S, SF150-S, SF155-S, SF160-S, SF165-S, SF170-S* [online]. Available: <http://www.solar-frontier.eu/fileadmin/content/downloads/modules/en/20141030/product-overview-s-series-english.pdf> (15.12.2016)